MICROCRYSTALLINE, NANOCRYSTALLINE, POROUS,
AND COMPOSITE SEMICONDUCTORS

Effect of Conditions of Electrochemical Etching on the Morphological, Structural, and Optical Properties of Porous Gallium Arsenide

P. V. Seredin[a]*, **A. S. Lenshin**[a], **A. V. Fedyukin**[a], **D. L. Goloshchapov**[a], **A. N. Lukin**[a],
I. N. Arsentyev[b], and **A. V. Zhabotinsky**[b]

[a] *Voronezh State University, Voronezh, 394006 Russia*
[b] *Ioffe Institute, St. Petersburg, 194021 Russia*
*e-mail: paul@phys.vsu.ru
Submitted June 5, 2017; accepted for publication November 27, 2017

Abstract—The properties of porous GaAs samples produced by the electrochemical etching of single-crystal n-GaAs(100) wafers are studied by X-ray diffraction analysis, electron microscopy, and infrared and ultraviolet spectroscopy. It is possible to show that, by choosing the composition of the electrolyte and the conditions of etching, samples can be produced not only with different degrees of porosity and pore sizes (nanopores/micropores), but with another type of sample surface as well. The etching of n-GaAs(100) wafers under the conditions chosen in the study does not change the orientation of the porous layer with respect to the orientation of the single-crystal GaAs(100) substrate. At the same time, etching induces a decrease in the half-width of the diffraction peak compared to that for the initial wafer, a splitting of the phonon mode in the infrared spectra and a partial shift of the components in accordance with the parameters of anodic etching, and a change in the optical properties in the ultraviolet region.

1. INTRODUCTION

Over the last few decades, numerous methods for the production of porous semiconductor structures have been tested. Among these methods, electrochemical anodic etching is the most universal of those developed so far [1–3]. Its specific features, such as low temperature and the simplicity and low cost of application, make the method most attractive for the production of nanocrystalline porous materials on the basis of silicon and III–V binary semiconductors and their alloys [4–6]. Porous nanostructures electrochemically formed on the basis of GaAs are rather attractive materials for a wide range of applications [7], which is supported by the already known data reported in publications [8]. In recent years, nanoporous GaAs layers have been extensively used for the formation of a transitional buffer layer with a reduced elasticity coefficient in the production of heterostructures with a large mismatch between the lattice parameters in the heteropair. The use of porous GaAs layers for the production of antireflection layers of solar cells is no less relevant [2, 7].

It is well known that, by choosing an appropriate composition of the electrolyte, the configuration of the electrochemical etching cell, and the operation characteristics of etching, it is possible to attain the necessary parameters of porous GaAs layers. However, with all this, the quality of currently produced porous GaAs layers is rather far from perfect and is not always suitable for further epitaxy. It is well known that, upon the electrochemical etching of n-GaAs, the pore density and size and the structure of the porous layer are highly dependent on the dopant density and the crystallographic orientation of the initial wafer. Therefore, the development of the production technology and studies of the structural and optical quality of the porous GaAs layer in relation to the composition of the electrolyte play an important role in the achievement of success.

Thus, the purpose of the study is to explore the properties of porous GaAs produced by the electrochemical etching of single-crystal wafers. This is done by X-ray diffraction (XRD) analysis, electron microscopy, and infrared (IR) and ultraviolet (UV) spectroscopy.

2. EXPERIMENTAL

The substrate was an n-GaAs wafer with mirror-polished sides. The wafer was doped with silicon to the concentration $n = 10^{18}$ cm^{-3}. Before electrochemical etching, the samples were placed into am ultrasonic bath, in which the samples were degreased in acetone,

Table 1. Conditions of sample production

Sample	Current density, mA cm^{-2}	Composition of HF : C_3H_7OH electrolyte
A13	25	1 : 4
A15	75	1 : 4
A17	25−75	1 : 6

isopropanol, and ethanol. Thereafter the samples were washed in distilled water. Then we removed the natural oxide layer from the GaAs wafer surface by etching in $NH_4OH : H_2O_2 : H_2O$ (1 : 1 : 10), $HCl : H_2O_2 : H_2O$ (1 : 1 : 20), and $NH_4OH : H_2O$ (1 : 5) solutions for 30, 100, and 30 s, respectively.

A porous layer on the treated GaAs wafers was formed with the use of a specially designed electrochemical etching cell with a uniquely shaped electrode that provided a uniform distribution of the field over the wafer surface. This made it possible to attain homogeneous morphological properties and characteristics of the sample over its surface. In the first part of the experiment, the composition of the electrolyte corresponded to HF : C_3H_7OH = 1 : 4. The current density at the electrodes was varied in the range 25–100 mA cm^{-2}. For the second part of the experiment, we chose the HF : C_3H_7OH = 1 : 6 electrolyte. The range of variations in the current density was 25–75 mA cm^{-2}.

Diagnostics of the porous GaAs layers fabricated in the study was performed by X-ray diffraction (XRD) analysis, using a DRON4-07 diffractometer with a Co tube. The quality of the surface was analyzed using a Libra 120 Carl Zeiss electron microscope. The IR reflectance spectra in the region of phonon resonance in GaAs were obtained with a Vertex-70 Bruker IR Fourier spectrometer equipped with an attachment operating in the reflection mode of measurements with a variable angle of incidence of radiation. The angle of incidence could be varied in a wide range. The optical properties of the samples were studied in the range 190–900 nm by UV spectroscopy, using a LAMBDA 650 Perkin Elmer instrument equipped with a URA universal attachment that makes it possible to obtain reflectance spectra in the range of angles of incidence from 8° to 80°. At the same time, the working design of the attachment allows one to determine the absolute reflectance. Here, the reflectance spectra were recorded at the angle of incidence 67°. To record the photoluminescence (PL) spectra of the porous layer, we used an improved USB4000-VIS-NIR (Ocean Optics) optical-fiber spectrometer connected to a computer. The engineering solution suggested to improve the optical scheme allowed us to substantially reduce the losses of the luminescence signal when transferred to the spectrometer and to exclude frequency-dependent losses. For the PL excitation

sources, we used a laser module with an emission peak at 532 nm. The radiation power density was no higher than 20 mW cm^{-2}. The time resolution of the system was defined by the resolution of the spectrometer and corresponded to 3.8 ms. To cut out the long-wavelength region of emission from laser diodes and to set aside the fluorescence emission, we used appropriate interference optical filters (ThorLabs).

3. RESULTS

As noted above, the choice of the conditions of anodic etching (the composition of the electrolyte and the current density delivered to the electrodes in order to produce a uniformly etched GaAs layer with different degrees of porosity) is the basic problem posed in the study. For the first part of the experiment, we used an electrolyte with the composition HF : C_3H_7OH = 1 : 4. This composition of the electrolyte attracted our attention due to its availability. In addition, it has already been shown [5] that, with such composition of the electrolyte, it is possible to produce nanoporous GaAs layers. The current density delivered to the electrodes was varied in the range 25–100 mA cm^{-2}. It should be noted that, as the time of electrochemical etching is increased, a dark film is formed at the sample surface and, as the current density is increased to $J \geq 50$ mA cm^{-2}, a thick porous layer that can be easily separated from the substrate can be formed. At $J = 100$ mA cm^{-2}, this layer may break up into powder even during etching. The processes observed in the study are similar to those described in [6], although the compositions of electrolytes are different.

In the second part of the experiment, we changed the composition of the electrolyte: specifically, we increased the fraction of alcohol in the composition of the electrolyte. The composition came to correspond to the HF : C_3H_7OH = 1 : 6 solution. We changed the limits of variations in the current density: we lowered the upper limit to 75 mA cm^{-2}. Such changes allowed us to noticeably reduce erosion of the surface (by several times) and to obtain a new optimal result of etching.

Based on the experimental results, we selected the samples most promising for studies. The conditions of the formation of these samples are given in Table 1.

To determine the phase composition and structural quality of the layers after synthesis of the samples, we studied the materials by the XRD method. Figure 1 shows the survey diffraction patterns of the samples and the single-crystal GaAs substrate. As can be seen from the XRD data, the diffraction patterns of all of the samples exhibit only the (200) and (400) diffraction reflections characteristic of (100)-oriented single-crystal GaAs. First, this observation suggests that, under the conditions of etching chosen for the experiment, no porous polycrystalline layer is formed, which is generally typical of similar processes of the forma-
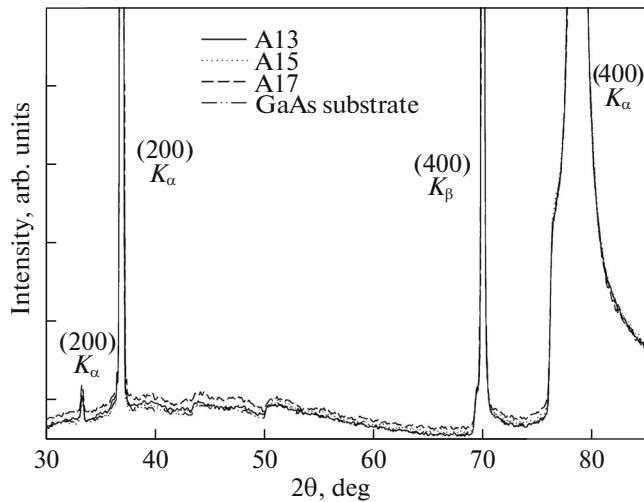
Fig. 1. XRD results.

Fig. 2. Diffraction profiles of (600) $K_{\alpha 1}$ reflections for the single-crystal substrate and samples with a porous layer.

tion of porous silicon [9, 10]. Second, the experimental data show that the layer formed by anodic etching possesses the same (100) crystallographic orientation as that possessed by the single-crystal GaAs substrate. It was possible to judge the structural quality of the porous GaAs layer by analyzing the (600) $K_{\alpha 1}$ reflection line of GaAs in the region of large angles ($2\Theta \sim 143°$). Figure 2 shows the profiles of these (600) lines for the single-crystal substrate and the samples with a porous layer. Analysis of the half-width of the (600) $K_{\alpha 1}$ reflection (see Table 2) shows that the formation of a porous layer does not deteriorate the structural quality of the sample. In contrast, an increase in the current density upon etching and the choice of the composition of the electrolyte yields a decrease in the half-width of the diffraction maximum compared to the corresponding parameter for the single-crystal substrate. This effect is a result of the etching-out of imperfect regions in the single-crystal wafer.

The processes of the formation of pores and the surface morphology of porous n-GaAs samples were studied by scanning electron microscopy (SEM). Figure 3 shows the micrographs of some regions of the porous layer (cleavages) of the samples under study. Specifically, Figure 3a shows the surface morphology of sample A13. From Fig. 3, it can be seen that the conditions of anodic etching chosen allow us to produce a 10-µm-thick porous layer with pronounced valleys at the surface, up to 1 µm in diameter, and with a system of small pores within the porous layer. At the same time, an increase in the current during etching makes it possible to form a more pronounced nanoporous layer on n-GaAs, with a system of pores oriented perpendicularly to the surface, as in the case of sample A15, whose cleavage is shown in Fig. 3b. In structure and morphology, the type of experimentally produced nanoporous GaAs layer is similar to that of the layer formed upon the anodic etching of Si [11].
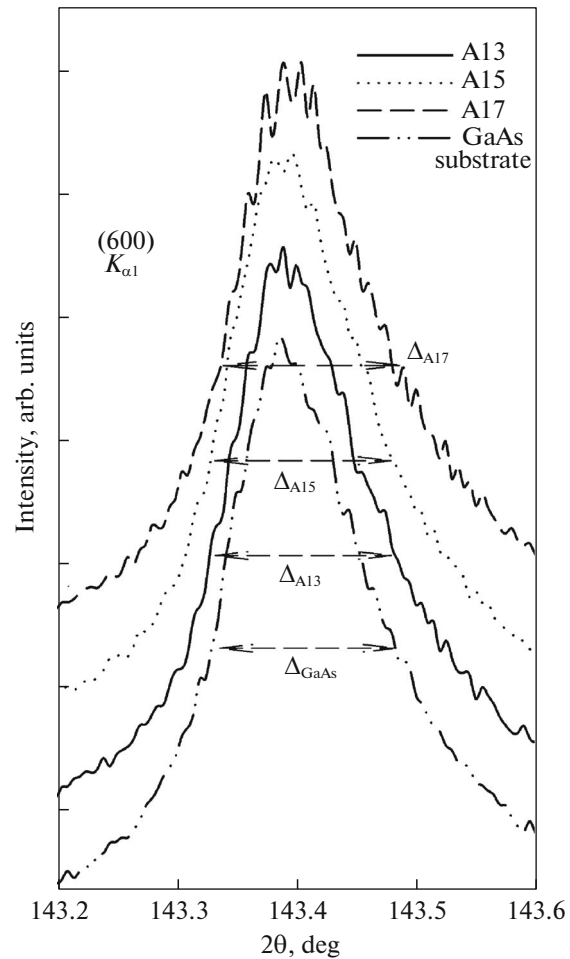
The result obtained in the second stage of the experiment (Fig. 3c) here seems no less interesting. The choice of the conditions of anodic etching allowed us to form regular single-crystal GaAs polyhedrons at the surface of the GaAs wafers; the polyhedrons are spaced from each other by comparable distances and arranged with the same density per unit area (Fig. 3c).

To study the fine properties of the crystal lattice and to judge the structural quality of the porous layers, we employed IR reflectance spectroscopy, which provides a means for drawing conclusions regarding not

Table 2. XRD results

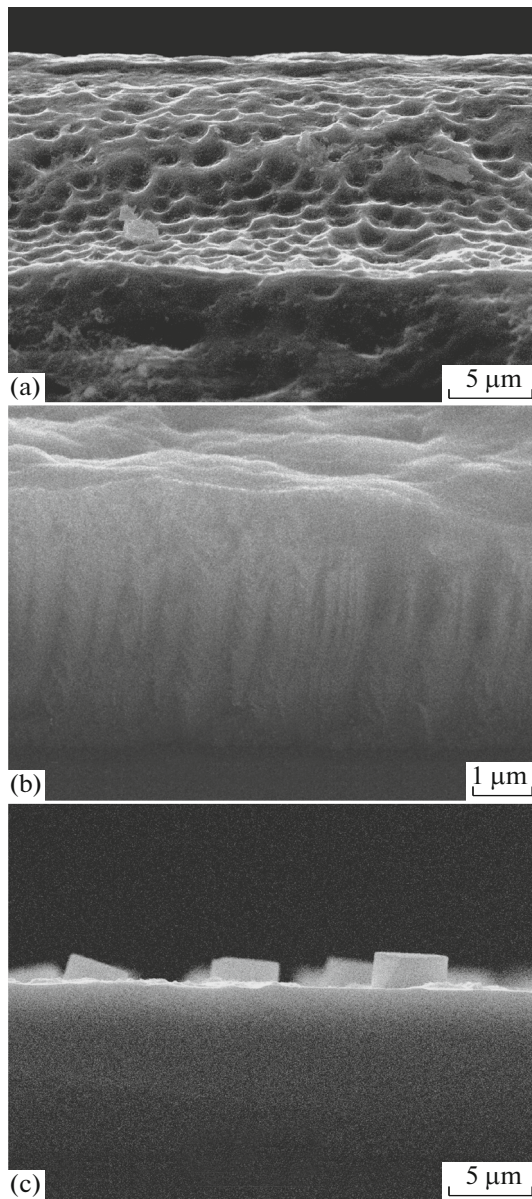| Sample	Half-width of peak, deg
GaAs substrate	$\Delta_{\text{GaAs}} = 0.152$
A13	$\Delta_{\text{A13}} = 0.146$
A15	$\Delta_{\text{A15}} = 0.137$
A17	$\Delta_{\text{A17}} = 0.137$

Fig. 3. SEM data for cleavages of samples (a) A13, (b) A14, and (c) A17 produced by the anodic etching of GaAs(100).

Fig. 4. IR reflectance spectra in the region of the phonon resonance for structures produced by anodic etching and the GaAs(100) substrate.

only the composition of the material, but internal lattice strains, to which the method is very sensitive [12, 13], as well. As can be seen from the experiment, the spectra of all of the samples contain only the high-intensity vibration mode corresponding to Ga–As vibrations. In addition, low-intensity modes localized in two regions appear in the reflectance spectra of the samples with a porous layer (see Fig. 4). Specifically, the transverse modes localized at 335–315 cm^{-1} and clearly seen in the spectra of samples A15 and A17 most probably correspond to vibrations in Ga$_x$O$_y$ oxides formed by etching of the initial single-crystal wafer. This result is consistent with the data reported in [14]. As concerns the range 220–215 cm^{-1}, in which
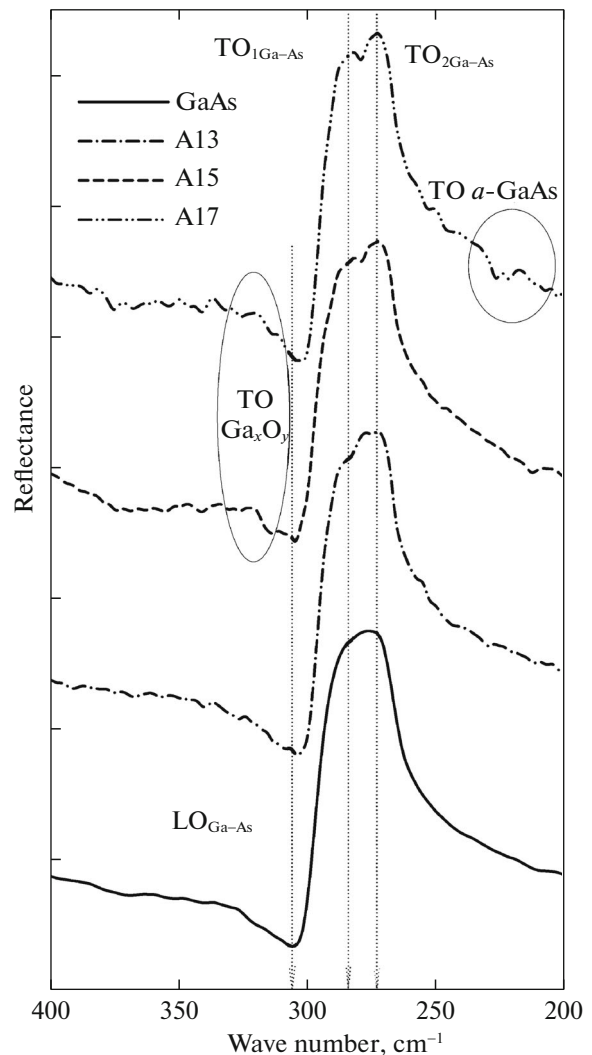
we observe a low-intensity vibration in sample A17 produced in the second stage of the experiment, the data of [15] show that this vibration is a consequence of the formation of a thin amorphous GaAs layer (*a*-GaAs) upon anodic etching on the *n*-GaAs(100) wafer.

Analysis of the experimental data shows that the shape of the principal phonon vibration of single-crystal GaAs (see Fig. 4) and the longitudinal and transverse phonon frequencies, $\omega_{LO} = 291$ cm^{-1} and $\omega_{TO} = 267$ cm^{-1} determined here coincide with the well-known data reported in publications [16, 17] and with the results of our previous studies [18, 19]. In the case of samples with a porous layer, the shape of the phonon spectrum experiences some change. In the reflectance spectrum, we can clearly see not only splitting of the phonon mode into the TO$_{1\,Ga–As}$ and TO$_{2\,Ga–As}$
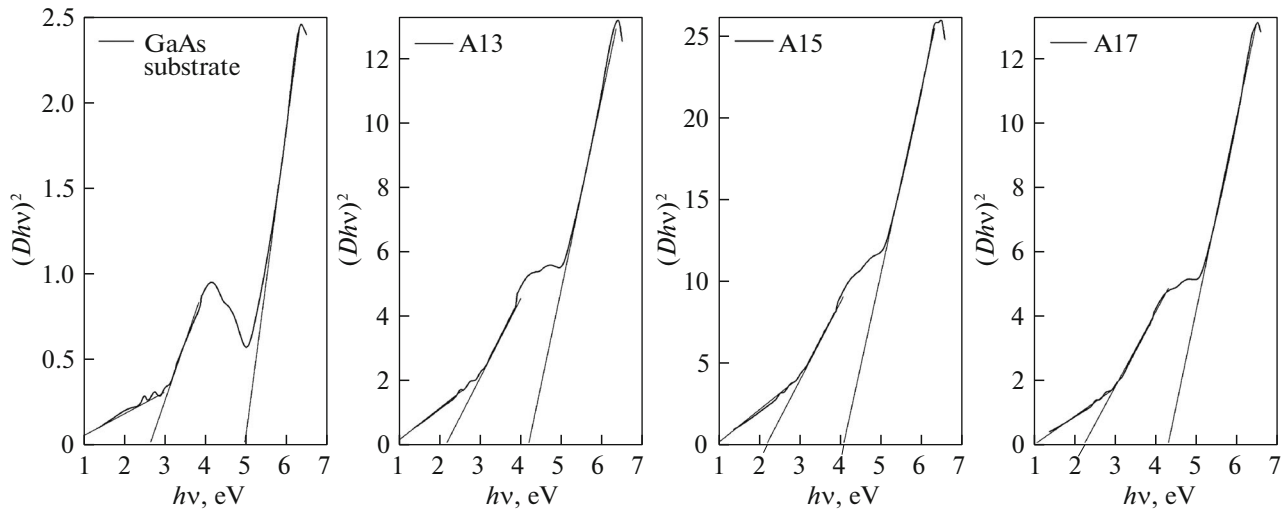
Fig. 5. Dependences of $(D \cdot h\nu)^2$ on the photon energy $h\nu$ for the structures produced by anodic etching and the GaAs(100) substrate.

components, but also a frequency shift of these components in accordance with the parameters of anodic etching. It should be noted that the splitting of the phonon mode into components correlates with the XRD data, specifically, with the half-width of the (600) $K_{\alpha 1}$ diffraction reflection peak. It can be clearly seen that, as the splitting of the phonon mode increases, the amplitude of the (600) $K_{\alpha 1}$ reflection decreases. The appearance of some vibrations in the IR reflectance spectrum is most probably caused by the localization of optical phonons in the layer created by anodic etching, similarly to how it happens in the case of superlattices [20].

To study the optical properties in the UV region for layers formed by anodic etching, we used a previously developed approach based on the reflection mode of recording [21−23]. This approach provides a means for gaining information on films/layers, deposited/formed on optically denser bulk substrates.

The transmittance−reflectance spectra of the samples under study were obtained at a 45° angle of incidence of electromagnetic radiation in the range 190−900 nm. To clarify the mechanisms of optical absorption in the layers formed by electrochemical etching, we made use of the possibilities of the OPUS Bruker software and took into account the Lambert−Bouguer formula $T = \exp[-D]$, where T is the transmittance and D is the optical density. On this basis, we reconstructed the transmittance−reflectance spectra into the absorption spectra.

Figure 5 shows the dependences of the quantity $(D \cdot h\nu)^2$ on the photon energy $h\nu$ for single-crystal GaAs and for the samples produced by electrochemical etching. The dependences were calculated from the specular reflectance spectrum by the Kramers−Kronig relations [24].

Graphical analysis of the dependences of $(D \cdot h\nu)^2$ on the photon energy allowed us to distinguish some regions of the linear dependence of $(D \cdot h\nu)^2$ on the photon energy. This can be indicative of direct allowed transitions in the corresponding spectral regions (Fig. 5). From linear extrapolation of the corresponding portions of the dependences to zero, it was possible to determine the energies of direct transitions characteristic of the samples. The energies of transitions determined for the samples under study by the above-described procedure are given in Table 3.

Analyzing the results obtained in the study and the data available in publications [25], we can state that, in the spectrum of the single-crystal substrate, we observe two types of direct transitions with the energies 2.90 and 5.03 eV, of which the former corresponds to the transitions $\Lambda_3 \to \Lambda_1$ and the latter (higher energy) to the transitions $X_5 \to X_1$. As to the spectra of samples with a porous layer produced by anodic etch-

Table 3. Energies of direct interband transitions in the spectra of the samples

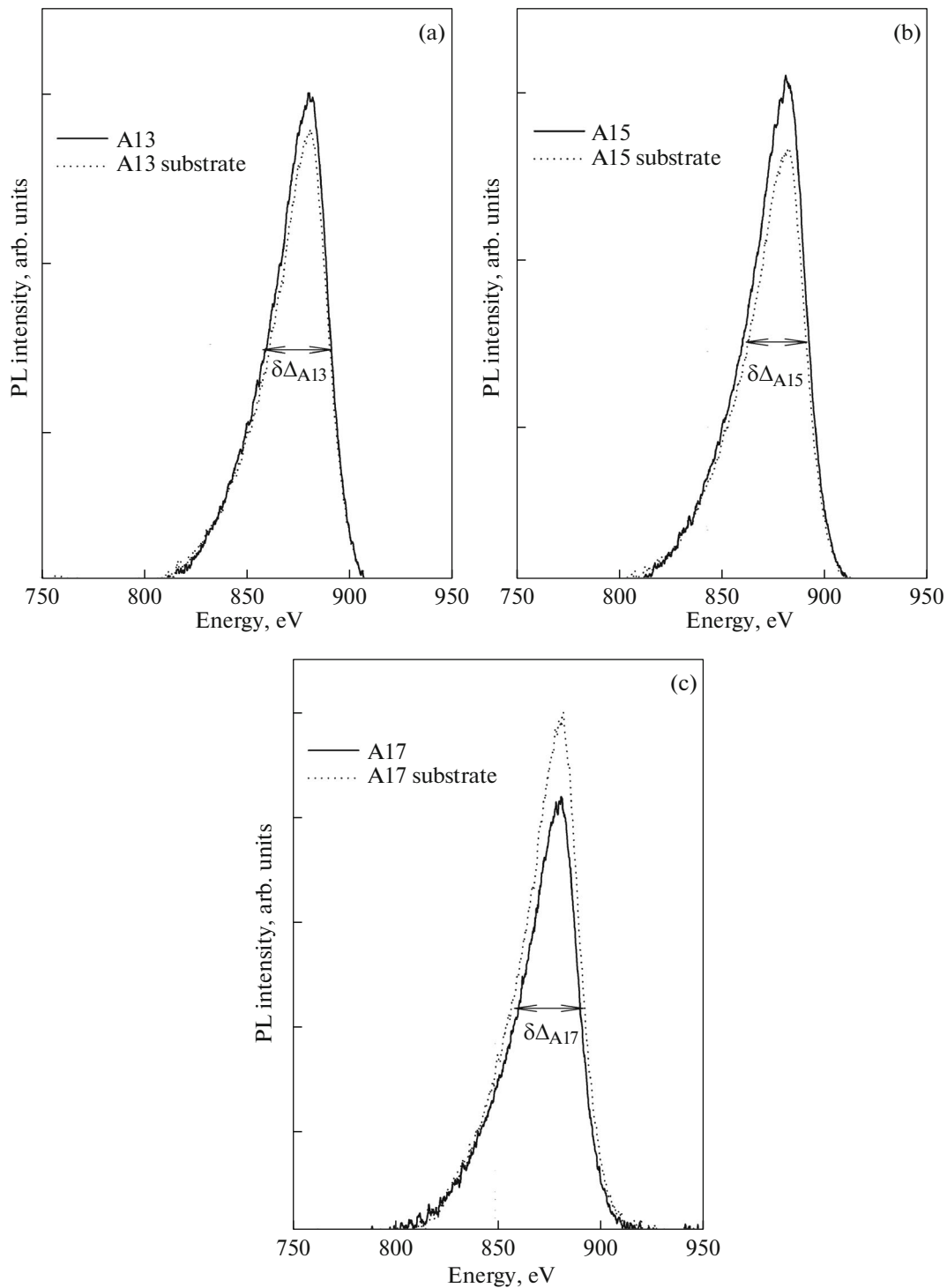| Sample	Type and energy of transition, eV	
GaAs substrate	$\Lambda_3 \to \Lambda_1$ 2.90 eV	$X_5 \to X_1$ 5.03 eV
A13	$\Gamma_{15} \to \Gamma_{15}$ 2.20 eV	$L_3 \to L_1$ 4.25 eV
A15	$\Gamma_{15} \to \Gamma_{15}$ 2.20 eV	$L_3 \to L_1$ 4.05 eV
A17	$\Gamma_{15} \to \Gamma_{15}$ 2.20 eV	$L_3 \to L_1$ 4.03 eV

Fig. 6. PL spectra of the structures produced by anodic etching in comparison with the PL spectrum of the GaAs(100) wafer used for the production of the samples.

ing of the initial wafer, these spectra involve two types of transitions as well, with the energies ~2.2 and ~4.15 eV. According to the data reported in publications [25], these energies correspond to the direct transitions $\Gamma_{15} \rightarrow \Gamma_{15}$ and $L_3 \rightarrow L_1$ from the valence band to the conduction band. It is quite evident that the anodic etching of n-GaAs brings about different optical properties in the UV region compared to the corresponding properties of initial single-crystal n-GaAs.

It is well known that a change in the stoichiometric composition in the porous GaAs layer produced by electrochemical etching is bound to influence the energy characteristics, i.e., PL spectra of the layer. The use of PL spectroscopy in order to analyze the electron structure of materials, to determine the band gap, and to investigate impurity levels, as well as to study recombination mechanisms and to determine the quality of materials, seems to be the optimal approach.

Figure 6 shows the PL spectra obtained for the samples under study and for the single-crystal GaAs(100) substrate used for the production of the sample. The spectra are recorded at room temperature under identical conditions and shown in Fig. 6 without normalization. From the experimental results, it can be seen that, in the spectra of all of the samples, there is one emission peak at the photon energy ~1.43 eV corresponding to band-to-band transitions in GaAs. However, it is noticeable that the PL intensity for the layer produced by anodic etching depends on the conditions of fabrication of the sample. Specifically, the experiment shows that, in the case of the fabrication of microporous and nanoporous GaAs layers, the PL intensity increases, with a slight decrease in the half-width of the PL band ($\delta\Delta A_{13} \sim 1.5$ nm, $\delta\Delta A_{15} \sim 1.5$ nm). In the case of nanoporous GaAs, the emission is enhanced by more than 20% compared to the PL emission from the initial wafer. The experimentally observed change in the PL spectra of samples with a porous layer is caused by a decrease in the absorption at free charge carriers (electrons), whose number in the porous surface layer is decreased, and by a reduction in the surface recombination in the porous layer.

At the same time, attention should be drawn to the PL spectra of sample A17. At the surface of this sample, there are regular single-crystal GaAs polyhedrons formed by electrochemical etching. For this sample, the PL intensity is noticeably (~19%) lower compared to the PL intensity of the initial GaAs(100) wafer. This fact is most probably a consequence of the formation of an amorphous a-GaAs layer and a Ga_xO_y oxide phase responsible for the enhancement of nonradiative recombination processes at the sample surface.

4. CONCLUSIONS

The XRD technique, electron microscopy, and IR and UV spectroscopy are applied to studies of the properties of porous GaAs samples produced by the electrochemical etching of single-crystal n-GaAs(100) wafers. It is shown that, by choosing the composition of the electrolyte and the conditions of etching, it is possible to produce samples not only with different degrees of porosity and pore sizes (nanopores/micropores), but with another type of sample surface as well. An increase in the mass fraction of alcohol in the composition of the electrolyte and a decrease in the current in the etching cell makes it possible to noticeably reduce surface erosion (by several times) and to form regular single-crystal GaAs polyhedrons at the wafer surface. The etching of n-GaAs(100) wafers under the conditions chosen in the study does not change the orientation of the porous layer with respect to the orientation of the single-crystal GaAs(100) substrate. At the same time, the etching induces a decrease in the half-width of the diffraction peak compared to that in the initial wafer, splitting of the phonon mode in the IR spectra and a frequency shift of the components (with consideration for the parameter of anodic etching), and a change in the optical properties in the UV region. The conditions of electrochemical anodic etching influence the PL band intensity in the sample and allow an increase in the luminescence efficiency by more than 20%.

The data obtained in the study can be used to develop the technology of the production of porous GaAs layers with specified structural, morphological, and optical properties.

REFERENCES

1. M. Naddaf and M. Saad, J. Mater. Sci. Mater. Electron. **24**, 2254 (2013).
2. G. Flamand and J. Poortmans, Phys. Status Solidi A **202**, 1611 (2005).
3. A. I. Belogorokhov, S. A. Gavrilov, I. A. Belogorokhov, and A. A. Tikhomirov, Semiconductors **39**, 243 (2005).
4. P. Schmuki, D. J. Lockwood, H. J. Labbé, and J. W. Fraser, Appl. Phys. Lett. **69**, 1620 (1996).
5. A. Dyadenchuk, Int. J. Mod. Commun. Technol. Res. **2**, 5 (2014).
6. D. N. Goryachev and O. M. Sreseli, Semiconductors **31**, 1192 (1997).
7. Y. A. Bioud, A. Boucherif, A. Belarouci, E. Paradis, D. Drouin, and R. Arès, Nanoscale Res. Lett. **11**, 446 (2016).

8. A. Lebib, E. Ben Amara, and L. Beji, J. Lumin. **188**, 337 (2017).

9. A. S. Len'shin, V. M. Kashkarov, P. V. Seredin, B. L. Agapov, D. A. Minakov, and V. N. Tsipenyuk, Tech. Phys. **59**, 224 (2014).

10. A. S. Len'shin, V. M. Kashkarov, V. N. Tsipenyuk, P. V. Seredin, B. L. Agapov, and D. A. Minakov, Tech. Phys. **58**, 284 (2013).

11. A. S. Len'shin, V. M. Kashkarov, P. V. Seredin, D. A. Minakov, and E. P. Domashevskaya, Tech. Phys. **60**, 1096 (2015).

12. E. P. Domashevskaya, P. V. Seredin, A. N. Lukin, L. A. Bityutskaya, M. V. Grechkina, and I. N. Arsentyev, Surf. Interface Anal. **38**, 828 (2006).

13. P. V. Seredin, A. V. Glotov, A. S. Lenshin, I. N. Arsentyev, D. A. Vinokurov, and T. Prutskij, Semiconductors **48**, 21 (2014).

14. R. Bernal Correa, J. Montes Monsalve, A. Pulzara Mora, M. López López, A. Cruz Orea, and J. A. Cardona, Superf. Vacío **27**, 102 (2014).

15. N. K. Ali, M. R. Hashim, A. A. Aziz, H. A. Hassan, and J. Ismail, Electrochem. Solid-State Lett. **12**, K9 (2009).

16. P. M. Amirtharaj and D. G. Seiler, *Optical Properties of Semiconductors. Handbook of Optics*, Vol. 2: *Devices Measurements and Properties*, 2nd ed. (McGraw-Hill, New York, 1995).

17. S. Adachi, *Properties of Semiconductor Alloys: Group-IV, III−V and II−VI Semiconductors* (Wiley, Chichester, UK, 2009).

18. P. V. Seredin, A. V. Glotov, E. P. Domashevskaya, I. N. Arsentyev, D. A. Vinokurov, and I. S. Tarasov, Phys. B (Amsterdam, Neth.) **405**, 4607 (2010).

19. P. V. Seredin, A. V. Glotov, E. P. Domashevskaya, I. N. Arsentyev, D. A. Vinokurov, and I. S. Tarasov, Phys. B (Amsterdam, Neth.) **405**, 2694 (2010).

20. V. A. Volodin, M. D. Efremov, V. Y. Prints, V. V. Preobrazhenskii, B. R. Semyagin, and A. O. Govorov, JETP Lett. **66**, 47 (1997).

21. P. V. Seredin, A. S. Lenshin, V. M. Kashkarov, A. N. Lukin, I. N. Arsentiev, and A. D. Bondarev, Mater. Sci. Semicond. Proces. **39**, 551 (2015).

22. P. V. Seredin, V. M. Kashkarov, I. N. Arsentyev, A. D. Bondarev, and I. S. Tarasov, Phys. B (Amsterdam, Neth.) **495**, 54 (2016).

23. P. V. Seredin, A. S. Lenshin, D. L. Goloshchapov, A. N. Lukin, I. N. Arsentyev, and A. D. Bondarev, Semiconductors **49**, 915 (2015).

24. Yu. I. Ukhanov, *Optical Properties of Semiconductors* (Nauka, Moscow, 1977) [in Russian].

25. J. Tauc, Prog. Semicond. **9**, 87 (1965).

Translated by E. Smorgonskaya